European Polymer Journal 48 (2012) 1101–1109

Contents lists available at SciVerse ScienceDirect

European Polymer Journal

journal homepage: www.elsevier.com/locate/europolj

Polymerization-induced phase separation as a one-step strategy to self-assemble alkanethiol-stabilized gold nanoparticles inside polystyrene domains dispersed in an epoxy matrix

Hernán E. Romeo [a,*], Alejandro Vílchez [b], Jordi Esquena [b], Cristina E. Hoppe [a], Roberto J.J. Williams [a,*]

[a] Institute of Materials Science and Technology (INTEMA), University of Mar del Plata and National Research Council (CONICET), J.B. Justo 4302, 7600 Mar del Plata, Argentina
[b] Institute of Advanced Chemistry of Cataluña (IQAC), Spanish National Research Council (CSIC) and CIBER of Bioengineering, Biomaterials and Nanomedicine (CIBER-BBN), Jorge Girona Salgado 18-26, 08034 Barcelona, Spain

ARTICLE INFO

Article history:
Received 12 October 2011
Received in revised form 6 March 2012
Accepted 15 March 2012
Available online 27 March 2012

Keywords:
Polymerization-induced phase separation
Self-assembly
Nanoparticles
Polystyrene
Cross-linked polymer

ABSTRACT

The rational design of nanoparticle (NP)/polymer composites with advanced functional properties is based on controlling the distribution and self-assembly of NPs in the polymer matrix. In this study we report a new one-step strategy to produce the self-assembly of alkanethiol-stabilized Au NPs in one of the phases generated by polymerization-induced phase separation. The polymerization of a formulation composed of stoichiometric amounts of diglycidylether of bisphenol A (DGEBA) and *m*-xylylenediamine (*m*XDA), containing polystyrene (PS) and dodecanethiol-stabilized Au NPs as modifiers, produced the phase separation of PS and Au NPs into microdomains dispersed in the epoxy matrix. A subsequent phase separation and self-assembly of Au NPs took place inside the PS domains leading to an increase in their concentration in a region close to the interface as revealed by TEM images. SAXS spectra showed that NPs self-assembled as colloidal crystals with a body-centered cubic (bcc) structure. By an adequate selection of the amount of PS and the nature of the epoxy precursors, different morphologies of the final blend could be generated. This brings the possibility of controlling the dispersion and self-assembly of NPs in the final material.

1. Introduction

In recent years, interest in the preparation and characterization of nanostructured materials has grown due to their distinctive properties and potential technological applications [1,2]. Particularly, the combination of metallic nanoparticles (NPs) and polymers constitutes an attractive way for the design of nanocomposites with special functional properties [3–6], and potential applications in electronics [7], catalysis [8], or optics [9]. Individual NPs are frequently functionalized with organic ligands that impart colloidal stability and enable their dispersion in specific solvents [10]. For example, alkanethiolates (RS, where $R = C_nH_{2n+1}$ and S is a sulfur atom binding to the NPs surface) are used as stabilizers in some of the classic syntheses of Au NPs [11]. Depending on the ratio of the alkyl chain length and the metallic core diameter, alkanethiol-stabilized NPs can self-assemble as colloidal crystals with hcp, fcc, bcc, or other structures [12], with different sets of physical properties [13]. Hence, strategies leading to the generation of such assemblies constitute one of the main aspects of the so-called "bottom-up" approaches towards the development of advanced nanostructured functional materials. Incorporation of such assemblies in chemically and mechanically stable polymeric solid substrates, like crosslinked polymers, opens new and exciting ways for

* Corresponding authors.
E-mail addresses: hromeo@fi.mdp.edu.ar (H.E. Romeo), williams@fi.mdp.edu.ar (R.J.J. Williams).

0014-3057/$ - see front matter © 2012 Elsevier Ltd. All rights reserved.
http://dx.doi.org/10.1016/j.eurpolymj.2012.03.014

the development of materials for new technological applications.

Although it is possible to infuse NPs or generate them in situ in a crosslinked matrix [14], the presence of crosslinks normally restricts the possibility of their self-assembly into organized structures. Alternatively, by an appropriate selection of the stabilizing organic groups NPs may form stable solutions in the precursors of a crosslinked polymer [15]. However, in these cases a polymerization-induced phase separation takes usually place leading to the segregation of NPs from the crosslinked polymer [16]. A variety of structures formed by the self-assembly of NPs results from this process. For example, polyhedral oligomeric silsesquioxanes (POSS) can be segregated as crystalline platelets dispersed in an epoxy matrix [17]. Au NPs can be concentrated at the air-polymer interface as fractal aggregates with a hierarchical internal structure [18,19], or can generate micrometer nodules dispersed in the matrix [20]. Fractal aggregates provide a conductive path for antistatic films, optimizing the effect of a low initial concentration of NPs. Nodules exhibit a high dielectric constant that is useful for applications in electronics [20].

Another approach to self-assemble NPs inside a crosslinked polymer is to produce a multiphase material where NPs can be preferentially segregated to one of the phases. For example, a PS-*b*-PEO amphiphilic block copolymer can self-assemble in an epoxy matrix. TiO_2 NPs added to the initial formulation form dense arrays located at the interface between the epoxy matrix (containing the dissolved PEO block) and the microphase separated PS block [21]. Multiphase crosslinked polymers can also be obtained by curing a blend formed by a reactive monomer and a modifier that can phase separate during the course of polymerization. The possibility of employing these systems as hosts for the controlled dispersion and self-assembly of NPs is of great interest due to the variety of morphologies that can be generated. In this manuscript we report a simple one-step process for the encapsulation and self-assembly of dodecanethiol-stabilized Au NPs in microdomains of a linear polymer dispersed in an epoxy matrix. The idea was to use a linear polymer as a modifier of the initial formulation that can phase separate in the course of polymerization. If NPs have higher affinity for the linear polymer than for the epoxy they will be preferentially partitioned to the dispersed domains where they can self-assemble into a variety of structures. By modifying the size and shape of the phase formed by the linear polymer (e.g., by varying its molar mass or its initial concentration), the macroscopic distribution of self-assembled NPs in the crosslinked epoxy can be controlled. We have used this approach to encapsulate a liquid crystal inside polystyrene (PS) domains dispersed in an epoxy matrix, generating very efficient polymer dispersed liquid crystal (PDLC) films [22,23]. PS is a very interesting modifier of typical epoxy formulations because it exhibits a similar refractive index than the cured matrix leading to biphasic but transparent materials [24]. In this study we will show that dodecanethiol-stabilized Au NPs can be encapsulated and self-assembled inside PS domains dispersed in an epoxy matrix. To the best of our knowledge, this is the first report on the self-assembly of Au NPs encapsulated into dispersed domains of a linear polymer produced by polymerization-induced phase separation.

2. Experimental section

2.1. Materials

The selected epoxy monomer was based on diglycidylether of bisphenol A (DGEBA, DER 332 Dow Chemical), with a molar mass of 348.6 g/mol. The hardener was *m*-xylylenediamine (*m*XDA, Aldrich), which was blended with the epoxy monomer in a stoichiometric proportion (DGEBA/*m*XDA molar ratio = 2). The structures of both co-monomers are shown in Fig. 1. Polystyrene (PS, M_n = 28.400; PI = 1.07) was purchased from Polymer Source. Dodecanethiol (DDT), hydrogen tetrachloroaurate (III) trihydrate ($HAuCl_4{\cdot}3H_2O$, $\geqslant$49 wt.% as Au), tetraoctylammonium bromide and sodium borohydride were purchased from Aldrich and used as received to synthesize dodecanethiol-stabilized Au NPs. Tetrahydrofuran (THF, P.A. grade) and toluene (P.A. grade), were employed as solvents.

2.2. Synthesis of DDT-coated Au NPs

The synthesis was performed according to the Brust–Schiffrin method [11]. Briefly, 0.1 mmol of $HAuCl_4{\cdot}3H_2O$ were mixed with 244 mg of tetraoctylammonium bromide in 10 mL of toluene. The two-phase mixture was stirred until no coloration was observed in the aqueous phase. Then, 0.1 mmol of DDT were added to the organic solution. An excess of a freshly prepared sodium borohydride aqueous solution was subsequently added as a reducing agent. The as-synthesized DDT-stabilized gold NPs were then separated from unattached DDT by precipitation with ethanol (in a volume ratio respect to the toluene solution of 7:1), followed by centrifugation (8000 rpm). The wet product was finally dried at 40 °C and stored as a waxy solid at room temperature.

A TEM image of the Au NPs is shown in Fig. 2. The average size of gold cores is close to 2 nm.

2.3. Synthesis of nanocomposites by polymerization-induced phase separation

A solution containing 2.9 mg/mL DDT-stabilized Au NPs in THF was prepared. PS was dissolved in this solution in a mass ratio of PS:Au NPs of 10:1. Then, an amount of DGEBA (typically 200 mg) was added to give 10 wt.% PS (and 1 wt.% of Au NPs) in the final nanocomposite. THF was evaporated at 80 °C, the solution was cooled to room temperature and the stoichiometric amount of hardener (*m*XDA) was added. Samples were cast on silicon molds, cured at 80 °C for 1 h and post-cured at 130 °C for 30 min to attain complete conversion [25]. The resulting material was black and optically homogeneous.

For comparison purposes, two binary formulations were processed in the same way leading to DGEBA/*m*XDA matrices modified by 10 wt.% PS or by 1 wt.% Au NPs, respectively.

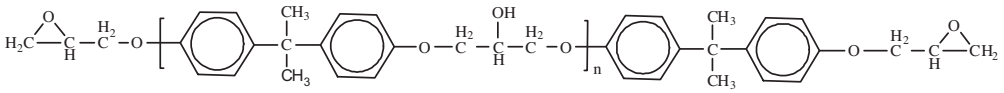

Diglycidylether of bisphenol A (n = 0.03)

(DGEBA)

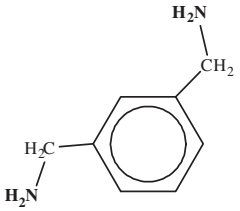

m-xylylenediamine

(mXDA)

Fig. 1. Chemical structures of DGEBA and *m*XDA.

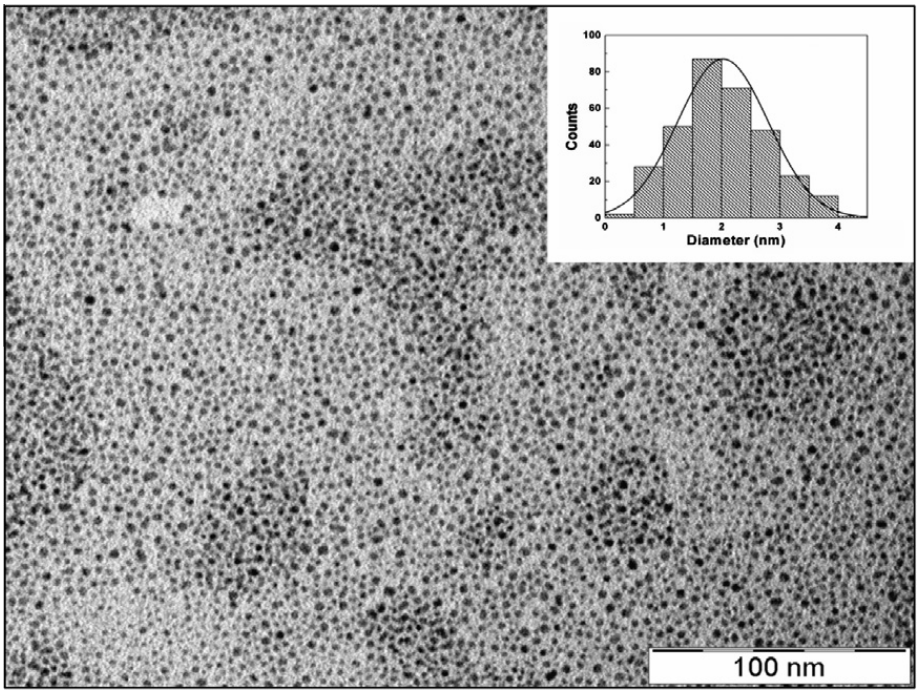

Fig. 2. TEM image of the Au NPs.

2.4. Characterization techniques

Near-infrared (NIR) spectroscopy was employed to determine conversion vs. time curves at 80 °C, for both the neat epoxy-amine formulation and the PS-modified system. A Genesis II-Mattson device, equipped with a heated transmission cell (HT-32, Spectra Tech) with quartz windows (32 mm diameter, 0,5 mm lead spacer) and a programmable temperature controller (Omega, Spectra Tech, $\Delta T = \pm 1$ °C), was employed. The conversion of epoxy groups was followed by measuring the height of the absorption band at 4530 cm^{-1} with respect to the height of a reference band at 4620 cm^{-1} [26,27].

The size distribution of the as-synthesized gold NPs was determined by employing a Jeol JEM 2011F transmission electron microscope (TEM) operated at an accelerating voltage of 200 kV. Samples were prepared by dropping 5 μL of the dispersion of NPs in THF on a copper grid coated with a carbon film. The same device was employed to observe the self-organization of the Au NPs inside the PS phase dispersed in the epoxy matrix. Ultrathin slices (about 60 nm thickness) were obtained with a Reichert

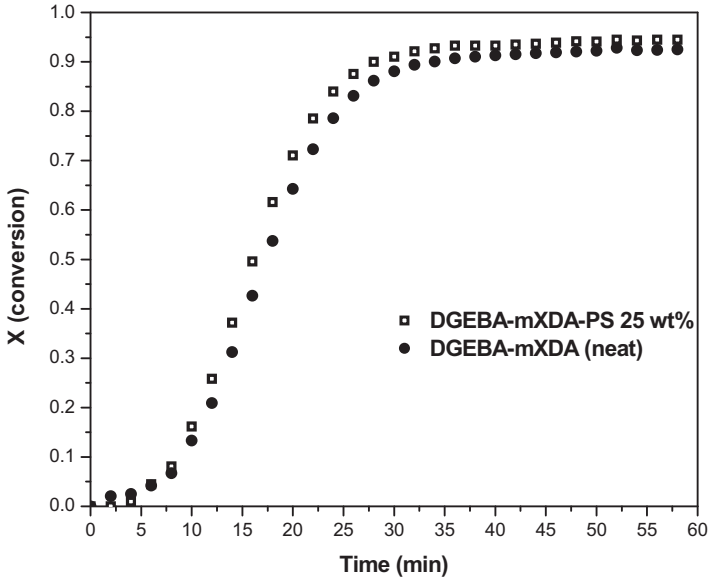

Fig. 3. Conversion of epoxy groups as a function of time at 80 °C.

Jung ultramicrotome (Seefeld, Germany) at room temperature, and supported on a copper grid covered with a carbon film.

Fracture surfaces of fully-cured blends (with and without Au NPs) were coated with a fine gold layer and observed by scanning electron microscopy (SEM, either Jeol JXA-8600 or Hitachi TM-1000).

Glass transition temperatures of fully-cured blends (with and without Au NPs) were determined by dynamic mechanical analysis (DMA 7, Perkin Elmer, Connecticut, USA) in a tensile configuration. Specimens 20 mm long, 3 mm wide and 0.3 mm thick, were tested.

The self-assembly of NPs produced in the nanocomposites was investigated by small-angle X-ray scattering (SAXS). Measurements were performed using a S3 MICRO instrument (Hecus X-ray Systems, Graz) equipped with a GENIX microfocus X-ray source and a FOX 2D point-focusing element (both from Xenocs, Grenoble). The scattering intensity (in arbitrary units) was recorded using PSD detectors (Hecus) as a function of the scattering vector $q = (4\pi/\lambda)\sin\theta$ (λ is the wavelength = 1.542 Å, and 2θ is the scattering angle). The samples were placed in a cell sealed with Kallebrat film (Kalle GmbH, Austria). The measurements were performed at 25 °C for 1 h, with the generator operating at 50 kV and 1 mA. The self-assembly process was also followed in situ by SAXS measurements. In this case, the initial formulation was placed in a cell sealed with Kallebrat film and measurements were carried out at 80 °C for 1 h, recording SAXS spectra every 15 min, with the generator operating at 50 kV and 1 mA.

3. Results and discussion

3.1. DGEBA/mXDA–PS blends

The polymerization-induced phase separation in these binary blends was discussed in a previous study [25]. At 80 °C, initial formulations containing 10–25 wt.% PS were homogeneous but phase separation took place very rapidly (after about 1 min reaction for the formulation containing 10 wt.% PS) [25]. Then, no dilution effect on the kinetics of the epoxy-amine reaction was recorded as shown in Fig. 3 for a blend containing 25 wt.% PS in comparison with the neat matrix. After 1 h reaction a maximum conversion close to 0.94 was attained as the reaction was arrested by vitrification. The 30-min post-cure at 130 °C enabled to reach full conversion within the experimental error.

Fig. 4 shows SEM images of cured blends containing 10 and 25 wt.% PS. In the blend containing 10 wt.% PS the dispersed domains correspond to PS. For the blend with 25 wt.% PS, a phase inversion was produced with epoxy/amine spherical domains dispersed in a PS matrix (this sample was disintegrated by immersion in THF). The DGEBA/*m*XDA–PS (10 wt.%) system was selected to prepare ternary blends with Au NPs.

3.2. DGEBA/mXDA–PS–Au NPs blends

The influence of adding PS to a blend of DGEBA/*m*XDA–Au NPs (1 wt.%) is shown in Fig. 5. Blends without PS showed a macroscopic separation of Au NPs in the cured material (Fig. 5a). The incorporation of 10 wt.% PS in the initial formulation led to a black-colored and optically homogeneous material (Fig. 5b).

Fig. 6 shows a SEM micrograph of the DGEBA/*m*XDA–PS (10 wt.%)–Au NPs (1 wt.%) cured blend. PS dispersed domains with an average size close to 4 μm are observed. Au NPs are located inside the PS domains as shown by TEM images (Fig. 7). In Fig. 7a, a high electronic contrast between the dispersed phase and the continuous epoxy matrix is clearly observed. This indicates that Au NPs were partitioned to the PS domains during the polymerization-induced phase separation process. The reason is the higher compatibility of the hydrophobic dodecyl chains with PS than with the polar epoxy/amine species. The magnified images (Fig. 7b and c) show that Au NPs are present

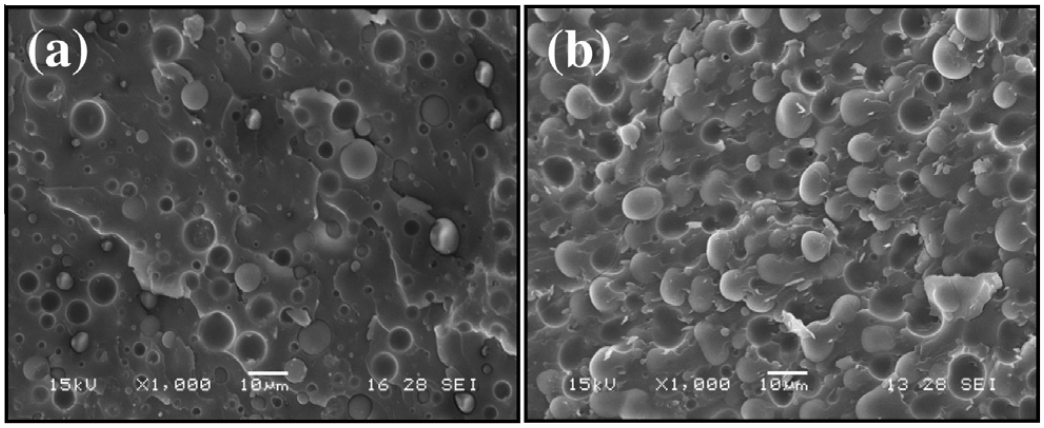

Fig. 4. SEM micrographs of DGEBA/*m*XDA–PS blends with different amounts of PS: (a) 10 wt.%, (b) 25 wt.%.

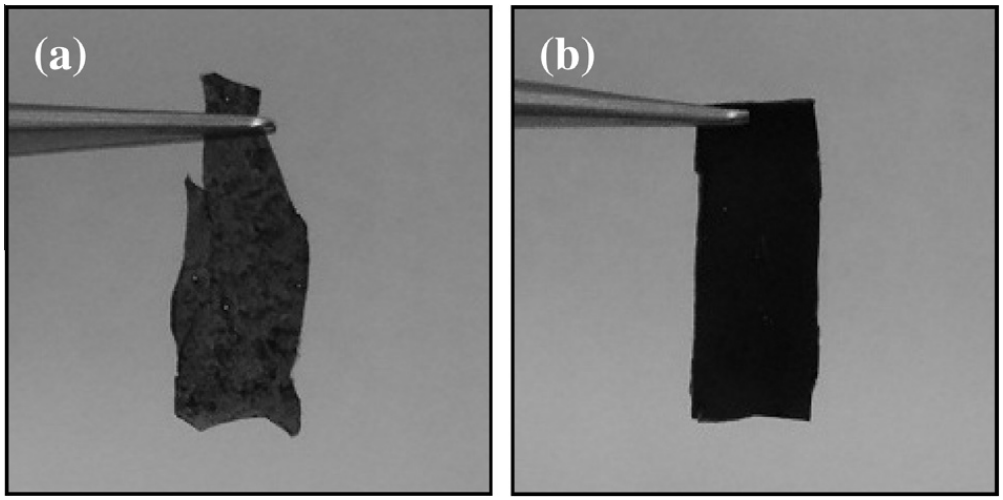

Fig. 5. Photographs of cured materials: (a) DGEBA/*m*XDA–Au NPs (1 wt.%), (b) DGEBA/*m*XDA–PS (10 wt.%)–Au NPs (1 wt.%).

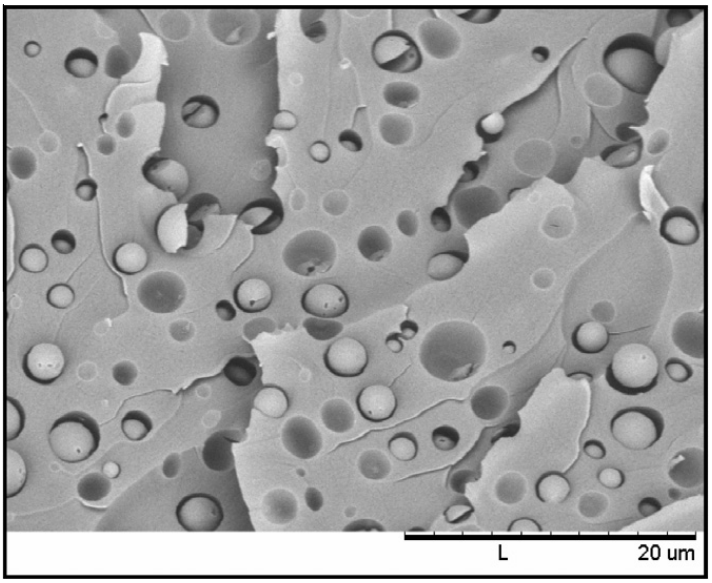

Fig. 6. SEM image of the DGEBA/*m*XDA–PS (10 wt.%)–Au NPs (1 wt.%) blend.

everywhere inside dispersed domains but they are more concentrated in a region close to the interface with the epoxy matrix. This means that a subsequent phase separation took place inside PS domains leading to a kind of diffuse

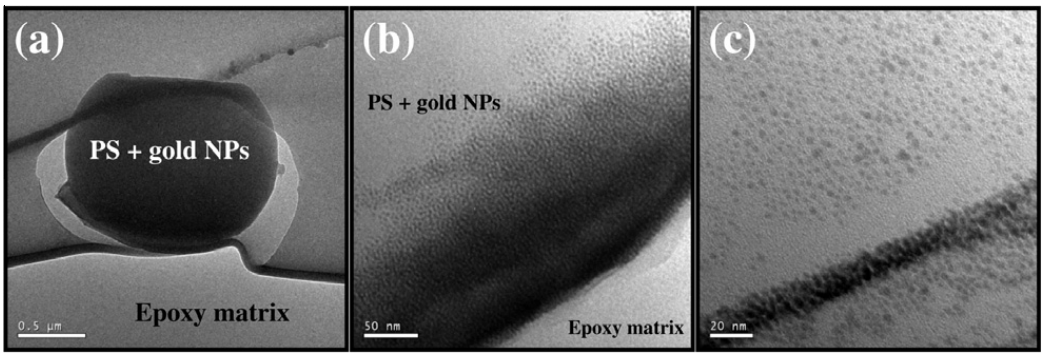

Fig. 7. Representative TEM images of the DGEBA/*m*XDA–PS (10 wt.%)–Au NPs (1 wt.%) blend. (a) Electronic contrast between PS–Au NPs phase and the epoxy matrix, (b) closer view of the PS–Au NPs/epoxy interface, (c) region inside a microsphere.

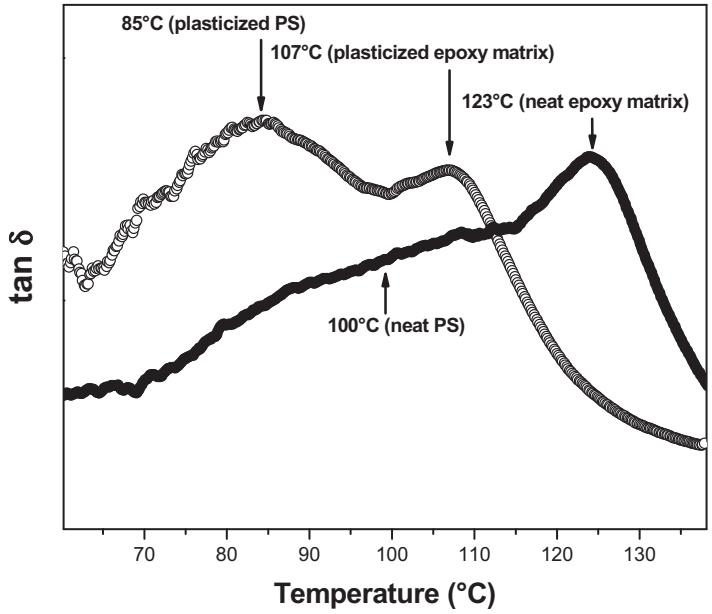

Fig. 8. Tan δ as a function of temperature corresponding to DGEBA/*m*XDA–PS (10 wt.%) (hollowed circles) and DGEBA/*m*XDA–PS (10 wt.%)–Au NPs (1 wt.%) (filled circles) cured blends.

shell of Au NPs located in the interfacial region. Although this is the final stage of the phase separation process, one can speculate on the way in which this morphology was generated. At the initial stage of the phase separation process, thermodynamics predicts that the composition of both phases does not correspond to the pure components [28,29]. Consequently, PS-rich and epoxy/amine-rich domains are initially generated. The PS-rich domains contain a significant fraction of epoxy/amine species while the matrix contains a residual fraction of PS. As polymerization goes on, mutual miscibility decreases and both phases tend to purify. Epoxy/amine species diffuse out of PS domains (or generate crosslinked sub-domains by a secondary phase separation process) and PS molecules from the matrix are incorporated to the dispersed domains (or generate new dispersed domains). Fig. 8 (filled circle curve) shows that the presence of Au NPs in the initial formulation produced an almost complete purification of the epoxy phase as revealed by the maximum of tan δ at 123 °C (the T_g value of the epoxy/*m*XDA matrix is ~120 °C). A similar purification effect is observed for the PS phase although in this case it was not complete and led to a broad peak possibly reflecting a gradient in its composition (this broad transition between both T_gs reveals the presence of an interface constituted by a blend of both components). TEM and DMA results enable to infer the way in which the observed morphology was generated. As a consequence of their non-polar coatings, Au NPs are more compatible with PS than with the epoxy-amine species. Therefore, as soon as a small conversion takes place, both components (Au NPs and PS) are segregated from the continuous epoxy phase together with a fraction of low molar mass epoxy-amine species (mostly monomers). The interesting fact is that the presence of Au NPs produced the complete segregation of PS from the bulk of the epoxy phase. However, as PS is not able to produce a homogeneous dispersion of the particular dodecanethiol-stabilized Au NPs used in this study, as soon as the segregated epoxy-amine species continue polymerization in the

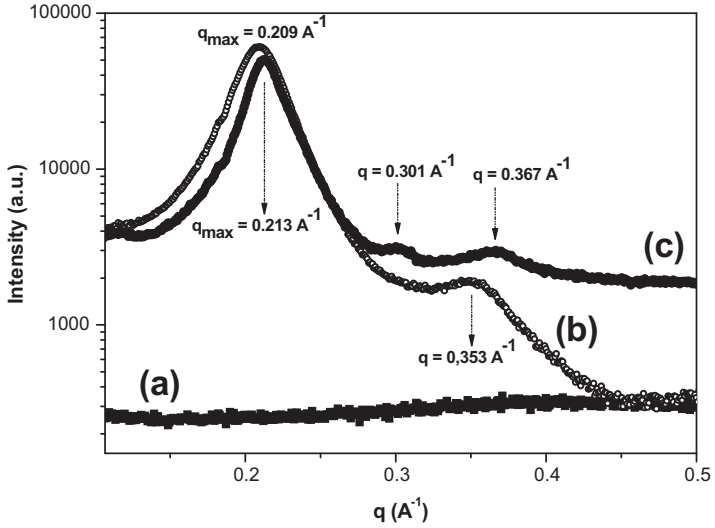

Fig. 9. SAXS spectra of: (a) DGEBA/*m*XDA–PS (10 wt.%) sample, (b) neat Au NPs, and (c) DGEBA/*m*XDA–PS (10 wt.%)–Au NPs (1 wt.%) blend.

dispersed phase there is a secondary phase separation of Au NPs inside the dispersed domains. As a consequence, NPs agglomerated in a region inside but close to the interface of PS dispersed domains (Fig. 7b), a process probably interrupted by vitrification of the PS phase.

The self-assembly of Au NPs inside PS domains was analyzed using SAXS (Fig. 9). As expected, the epoxy matrix containing 10 wt.% PS showed no peaks. On the other hand, the neat Au NPs deposited in the SAXS cell showed some organization (two scattering peaks) while the Au NPs self-assembled inside the PS domains exhibited a better organization manifested by the presence of three broad scattering peaks in a progression $q_0{:}\sqrt{2}q_0{:}\sqrt{3}q_0$, corresponding to a cubic structure.

The main factors determining the preferred crystalline structures usually observed for metallic NPs include not only their interactions, size and shape, but also their "softness", that represents the deformability of the stabilizing shell [12]. Depending on these factors, different kinds of nanostructures can be obtained, ranging from high-symmetry systems characterized by high coordination numbers (close-packing structures, mainly for "hard" objects) up to systems characterized by a strongly broken symmetry (mainly for "softer" entities). Generally, the particle-packing phenomenon involves a distinction between a central core (basically non-deformable and incompressible) and a concentric layer (corona) that is comparative softer than the hard core. Whetten et al. defined a dimensionless quantity (χ) that relates the geometric parameters of the particles and allows predicting the "softness" of the objects, based on the relationship between the thickness of the corona (L) relative to the radius (R) of the metallic core ($\chi = L/R$) [12]. Depending on the value of this parameter different crystalline structures are predicted [12]. In our case, taking $R \sim 1$ nm and $L = 1.6$ nm (the compact thickness of dodecyl chains between two neighboring NPs in a crystal) [12], gives $\chi \sim 1.6$. For this range of χ values, NPs should self-organize in a body-centered cubic (bcc) crystalline structure [12]. We can therefore assign the progression of the peaks observed in SAXS spectrum for the DGEBA/*m*XDA–PS (10 wt.%)–AuNPs blend to a bcc structure. For a bcc crystalline structure, allowed reflections require that the Miller indices verify the condition $h + k + l$ = even number. Therefore, the first allowed reflection is assigned to the planes (1 1 0), the second corresponds to the planes (2 0 0), and the third to the planes (2 1 1). The interplanar spacing is given by $d_{hkl} = a/(h^2 + k^2 + l^2)^{1/2}$ where a is the side of the cube. Using $d_{110} = 2\pi/q_{110} = 2.95$ nm, gives $a = 4.17$ nm. The distance between an individual NP and the eight equidistant neighbors in the bcc structure is equal to $(a\sqrt{3})/2 = 3.6$ nm. For NPs stabilized with dodecanethiol chains the thickness occupied by organic groups compressed between two NPs in the crystal is 1.6 nm [12]. Then, the diameter of the metallic core of NPs present in bcc crystals is 3.6–1.6 = 2.0 nm, which agrees with the average size observed in TEM images. Certainly, the size distribution of NPs did not allow a better ordering during the self-assembly process. As a summary, Au NPs become more concentrated inside PS regions close to the interfaces, and in such small regions the NPs self-assemble in an incipient bcc structure.

3.3. Monitoring the self-assembly of Au NPs during polymerization

The evolution of SAXS spectra during the cure at 80 °C of the DGEBA/*m*XDA–PS (10 wt.%)–Au NPs (1 wt.%) blend, is shown in Fig. 10. As phase separation took place very rapidly when temperature attained 80 °C, the first spectrum possibly corresponds to a sample just after the beginning of the phase separation. The broad scattering peaks at q values of 0.209 and 0.359 $Å^{-1}$, indicate that the self-assembly of Au NPs begins following phase separation. The organization improves continuously as inferred from the increase in the sharpness of the most intense peak and the generation of two small peaks (observed after 45 min) evidencing a short-range organization of a bcc structure.

It is interesting to point out that keeping the neat Au NPs in the SAXS cell at 80 °C for 1 h did not improve their

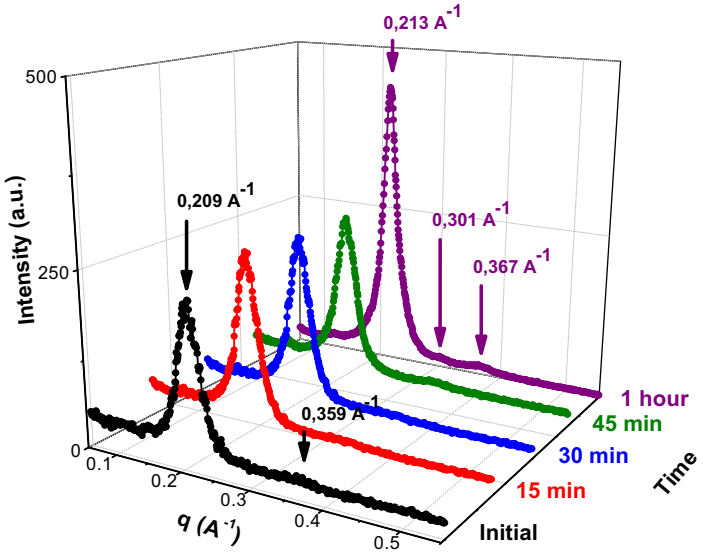

Fig. 10. SAXS spectra obtained for the cure at 80 °C of the DGEBA/*m*XDA–PS (10 wt.%)–Au NPs (1 wt.%) blend, as a function of time.

organization (SAXS spectra did not change). This evidences that there is an effect produced by the confinement of Au NPs near the interface in PS domains. This packing effect can be related to the small increase of the q value of the most intense scattering peak and the generation of an incipient bcc ordering.

4. Conclusions

By an adequate selection of the structure of the stabilizing organic groups, it is possible to disperse NPs in the precursors of a crosslinked polymer. However, in most cases a polymerization-induced phase separation takes place generating a macroscopic segregation of the NPs from the polymer matrix. This study has shown that a third component may be added to the initial formulation that can phase separate in the course of polymerization and produce the partitioning of NPs. In the present case, we used PS as the third component of the formulation. As a consequence of their non-polar coatings, Au NPs were more compatible with PS than with the epoxy-amine species. Therefore, as soon as a small conversion took place, both components (Au NPs and PS) were segregated from the continuous epoxy phase together with a fraction of low molar mass epoxy-amine species. The interesting fact is that the presence of Au NPs produced the complete segregation of PS from the bulk of the epoxy phase. However, as PS is not able to produce a homogeneous dispersion of the particular dodecanethiol-stabilized Au NPs used in this study, as soon as the segregated epoxy-amine species continued polymerization in the dispersed phase there was a secondary phase separation of Au NPs inside the dispersed domains. Nanoparticles self-assembled in a region inside but close to the interface of the PS dispersed domains as colloidal crystals with a short-range bcc structure.

The morphologies generated in the PS/epoxy blend may be varied with the amount of PS in the initial formulation (e.g., see Fig. 4), with its molar mass, with the selected cure schedule or by varying the nature of the hardener. The effect of changing the size of NPs and the nature of the stabilizing organic ligands can also be investigated. Work is in progress in this direction. In the general case, thermoplastic/thermoset blends can give place to a dispersed thermoplastic phase, a dispersed thermoset phase, two co-continuous phases or a combination of phase-in-phase morphologies [28,29]. This brings the possibility of controlling the way in which NPs will be dispersed in the final material. For example, percolating 3D paths of colloidal crystals may be generated and used for technological applications. Several other possibilities may be explored like the simultaneous use of different types of NPs (e.g., with optical and magnetic properties), and their preferential segregation to different phases, controlled by the nature of their stabilizing organic groups. But the most remarkable fact is that these complex morphologies can be obtained in one step by a polymerization-induced phase separation process.

Acknowledgments

We acknowledge the financial support of the National Research Council (CONICET, Argentina), the National Agency for the Promotion of Science and Technology (ANPCyT, Argentina), and the University of Mar del Plata. The financial support of the bilateral cooperation program "Luis Santaló" between Spain (CSIC) and Argentina (CONICET) is gratefully acknowledged.

References

[1] Philos WellerH. Trans R Soc London Ser A 2003;361:229.
[2] Uhlenhaut DI, Smith P, Caseri W. Adv Mater 2006;18:1653–6.
[3] Shenhar R, Norsten TB, Rotello VM. Adv Mater 2005;17:657–69.
[4] Althues H, Henle J, Kaskel S. Chem Soc Rev 2007;36:1454–65.
[5] Vaia RA, Maguire JF. Chem Mater 2007;19:2736–51.
[6] Alexandridis P, Tsianou M. Eur Polym J 2011;47:569–83.
[7] Balasz AC, Emrick T, Russell TP. Science 2006;314:1107–10.
[8] Luo J, Jones VW, Han L, Maye MM, Kariuki NN, Zhong CJ. J Phys Chem B 2004;108:9669–77.

[9] Liz-Marzán LM, Kamat PV, editors. Nanoscale Materials. Boston: Kluwer; 2003.
[10] Zhang T, Wu Y, Pan X, Zheng Z, Ding X, Peng Y. Eur Polym J 2009;45:1625–33.
[11] Brust M, Fink J, Bethell D, Schiffrin DJ, Kiely CJ. J Chem Soc Chem Commun 1995:1655–6.
[12] Whetten RL, Shafigullin MN, Khoury JT, Gregory Schaaff T, Vezmar I, Alvarez MM, Wilkinson A. Acc Chem Res 1999;32:397–406.
[13] Pileni MP, editor. Nanocrystals Forming Mesoscopic Structures. Weinheim: Wiley VCH; 2005.
[14] Ledo-Suárez A, Puig J, Zucchi IA, Hoppe CE, Gómez ML, Zysler R, et al. J Mater Chem 2010;20:10135–45.
[15] Soulé ER, Hoppe CE, Borrajo J, Williams RJJ. Ind Eng Chem Res 2010;49:7008–16.
[16] Soulé ER, Borrajo J, Williams RJJ. Macromolecules 2007;40: 8082–6.
[17] Di Luca C, Soulé ER, Zucchi IA, Hoppe CE, Fasce LA, Williams RJJ. Macromolecules 2010;43:9014–21.
[18] Zucchi IA, Hoppe CE, Galante MJ, Williams RJJ, López-Quintela MA, Matějka L, et al. Macromolecules 2008;41:4895–903.
[19] Gómez ML, Hoppe CE, Zucchi IA, Williams RJJ, Giannotti MI, López-Quintela MA. Langmuir 2009;25:1210–7.
[20] Ginzburg VV, Myers K, Malowinski S, Cieslinski R, Elwell M, Bernius M. Macromolecules 2006;39:3901–6.
[21] Tercjak A, Gutierrez J, Peponi L, Rueda L, Mondragon I. Macromolecules 2009;42:3386–90.
[22] Hoppe CE, Galante MJ, Oyanguren PA, Williams RJJ. Macromolecules 2004;37:5352–7.
[23] Hoppe CE, Galante MJ, Oyanguren PA, Williams RJJ. Mater Sci Eng C 2004;24:591–4.
[24] Hoppe CE, Galante MJ, Oyanguren PA, Williams RJJ. Polym Eng Sci 2002;42:2361–8.
[25] Zucchi IA, Galante MJ, Williams RJJ. Polymer 2005;46:2603–9.
[26] Min BG, Stachurski ZH, Hodgkin JH, Heath GR. Polymer 1993;34:3620–7.
[27] Poisson N, Lachenal G, Sautereau H. Vibr Spectrosc 1996;12:237–47.
[28] Williams RJJ, Rozenberg BA, Pascault JP. Adv Polym Sci 1997;128:95–156.
[29] Pascault JP, Williams RJJ. In: Paul DR, Bucknall CB, editors. Polymer Blends, Vol. 1: Formulation. New York, USA: Wiley; 2009. p. 379.